

The Hot Phonon Bottleneck Effect in Metal Halide Perovskites

T. Faber, L. Filipovic, and L.J.A. Koster*




Cite This: *J. Phys. Chem. Lett.* 2024, 15, 12601–12607



Read Online

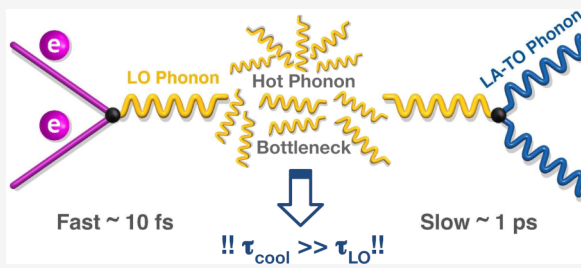
ACCESS |

 Metrics & More

 Article Recommendations

 Supporting Information

ABSTRACT: The hot phonon bottleneck (HPB) effect has been proposed as one of the main phenomena behind the slow cooling in metal halide perovskites. Even though consensus has been reached regarding its existence, open questions remain concerning the HPB's specific applicability and potential regarding hot carrier solar cell (HCSC) applications. We present a full investigation using ensemble Monte Carlo simulations of the HPB effect in metal halide perovskites (MHP). After describing the HPB effect in detail, we quantify how the HPB effect can extend carrier cooling times by orders of magnitude. We show how the HPB effect depends on carrier concentration, longitudinal optical (LO) phonon lifetime, and LO phonon frequency and connect these findings to how MHPs should be tuned concretely. Using ensemble Monte Carlo simulations, we can accurately model the interplay between carrier–phonon and carrier–carrier interactions up to high carrier density, yielding precise predictions regarding the HPB effect. This study provides important insights into the governing dynamics behind the HPB effect and shows how cooling times can be extended far beyond the phonon lifetime. Furthermore, it contributes to the discussion on cooling times in MHPs and their suitability for HCSC applications.



Metal halide perovskites (MHP) have had the center stage of photovoltaic research, since the moment they were first introduced.^{1,2} Due to their remarkable optoelectronic properties and defect tolerance, power conversion efficiencies of 26% have been reported.³ Additionally, MHPs have been a promising candidate for hot carrier solar cell (HCSC) applications, as numerous experimental reports have been published on slow hot carrier cooling.⁴ Slow carrier cooling is the crucial component for a material to qualify as an active layer in a HCSC.⁵ As was recently reviewed by Fu et al., a plethora of studies was published on the underlying intrinsic photophysics, considering several possible mechanisms such as the hot phonon bottleneck effect,^{6–16} polaron screening,^{17–21} Auger heating,^{7,14,15,22,23} band-filling,^{24,25} diminished electron–phonon coupling,²⁶ and an intrinsic phonon bottleneck effect.^{27,28}

Among these, the hot phonon bottleneck (HPB) effect is most widely accepted for its role in the extended cooling times.⁴ Generally, the physical picture behind the HPB effect is well understood for polar semiconductors.^{29–34} It was first reported for MHPs by Yang et al. in 2016.⁶ The HPB effect arises from a nonequilibrium population of longitudinal optical (LO) phonons,³⁵ and can be best understood when considering the full energy relaxation diagram:³⁶

1. carrier \rightarrow LO phonon. As MHPs are polar crystals, carriers interact strongly via LO-phonon coupling mediated via Coulomb interaction.^{37,38}
2. LO-phonon \rightarrow acoustic phonons. For cubic structures, this interaction takes place predominantly via the symmetric Klemens³⁹ decay (LO \rightarrow 2 LA phonons,

and subdominantly via the antisymmetric Ridley⁴⁰ decay (1 LO \rightarrow 1 LA + 1 TO phonon).⁴¹ LA and TO refer to longitudinal acoustic and transverse optical, respectively.

3. acoustic phonons \rightarrow thermal reservoir. Acoustic phonons conduct the energy in the form of heat away to the far-field region in the material.

As the LO-phonons are mainly produced around the zone center (stage 1), they have a rather low dispersion, causing them to largely remain in the photoexcited volume.⁴² If, at high excitation densities ($\rho > 10^{18} \text{ cm}^{-3}$), the carrier–LO phonon scattering rate (stage 1) is much higher than the LO phonon decay rate (stage 2), a nonequilibrium LO-phonon population can build up.⁴³

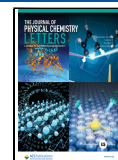
The HPB effect is a resultant effect arising from the discrepancy in decay times between carrier–phonon and phonon–phonon interactions. In Figure 1, a visualization of the effect is presented. The nonequilibrium LO phonon population, arising from the discrepancy, results in an increased probability of reabsorption by charge carriers. This is essentially how the HPB effect extends carrier lifetimes. LO phonons are swiftly reabsorbed, keeping carriers hot, instead of decaying further and converting carrier energy into heat. The HPB effect thus arises from the complex competitive interplay

Received: October 31, 2024

Revised: December 4, 2024

Accepted: December 6, 2024

Published: December 16, 2024



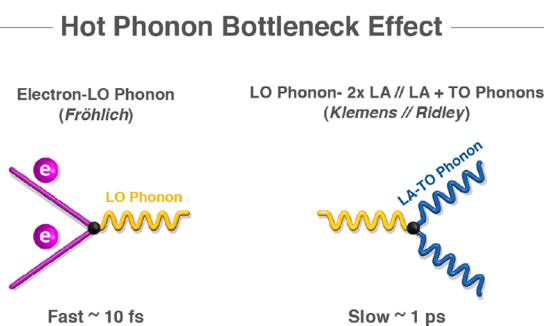


Figure 1. HPB effect arises due to a fast electron–phonon coupling rate, and a relatively slow phonon decay rate. In MHPs, the former is governed by the Fröhlich interaction, while the latter by the Klemens or Ridley decay.^{39,40}

between both the carrier–phonon and phonon–phonon interactions, and it is not only the phonon lifetime that determines the scale of the HPB effect.⁷ Therefore, it is not clear to what extent the HPB effect can elongate cooling times.

In this study, we show how the HPB effect can extend carrier cooling times far beyond LO phonon lifetime for metal halide perovskites, by observing the impact of the carrier concentration, LO-phonon lifetime, and LO phonon frequency. To model the particle dynamics through the entire cooling process, we use ensemble Monte Carlo (EMC) simulations.^{44–48} When dealing with nonequilibrium charge transport, the EMC method is a widely recognized numerical method to solve the Boltzmann transport equation.⁴⁹ In a previous study, we showed, using EMC, what the role is of thermalisation on the cooling dynamics of hot carriers in MHPs.⁵⁰

Our methodology allows us to accurately model the interplay between carrier–phonon and carrier–carrier interactions up to high carrier density, yielding precise predictions regarding the implications of the HPB effect. Moreover, by using ensemble Monte Carlo simulations, we are able to directly visualize our findings in a clear and concise way. For modeling the HPB effect, we use the algorithm developed by Lugli et al.⁵¹ It has been used together with the EMC for GaAs,^{52,53} for quantum wells in GaAs,⁵⁴ or InGaAs/InGaAsP;⁵⁵ however, it has never been applied in the context of perovskites.

Our model considers a single-mode approximation of the Fröhlich interaction. Even though this approximation holds well for certain types of perovskites,⁵⁶ it has been shown for MAPbI₃ that the consideration of multiple phonon modes is important in explaining transport properties such as the temperature dependence of the mobility.^{57,58} To solve this, one can consider an effective phonon mode coupling, composed of a mixture of multiple modes and resonating at a resultant frequency.^{59–62} However, the fundamental nature of the Fröhlich interaction that leads to the HPB effect is not altered by multiple phonon modes even though the coupling amplitude will be different. More important is the approximation regarding the weakly dispersive nature of the phonons, which in perovskites is shown to hold well.⁶³

As our findings relate to preferable concrete chemical compositions, we can formulate predictions on how perovskites should be tuned in order for them to maximally harness the full potential of the HPB effect. Our results show how extended cooling times can be achieved far beyond the LO

phonon lifetime, and give important insights into the governing dynamics behind the HPB in MHPs.

Our simulations were performed with the ensemble Monte Carlo code ViennaEMC,⁶⁴ consisting of carrier–LO-phonon interactions, and carrier–carrier scattering. We have integrated a fast multipole method (FMM) to compute the carrier–carrier interactions, for which we used the ScalFMM package.⁶⁵ For a more extensive overview on the ensemble Monte Carlo method we refer the reader to the [Supporting Information](#).

The transition rate for the carrier–LO-phonon or Fröhlich interaction is given by⁴⁷

$$S(k, k') = \frac{\pi e^2 \omega_0}{V} \left(\frac{1}{\epsilon_\infty} - \frac{1}{\epsilon_0} \right) \times \frac{1}{q^2} \left[N_q(\omega_0) + \frac{1}{2} \mp \frac{1}{2} \right] \delta(k' - k \mp q) \delta(E_k - E'_k \mp \hbar \omega_0) \quad (1)$$

where e is the elementary charge, ω_0 is the typical phonon frequency, V is the volume, and ϵ_∞ and ϵ_0 are the optical and static parts of the dielectric constant, respectively. The phonon occupation number is given by N_q for absorption (–) and $N_q + 1$ for emission (+).

The LO-phonon scattering rate for both absorption and emission is computed by performing an integration over q , or all final states.⁴⁴ One obtains:⁴⁴

$$\Gamma(E, E') = \frac{e^2 \sqrt{m^*} \omega_0}{\sqrt{2} \hbar} \left(\frac{1}{\epsilon_\infty} - \frac{1}{\epsilon_0} \right) \mathbf{F}(E, E') \left[N_q + \frac{1}{2} \mp \frac{1}{2} \right] \quad (2)$$

where m^* is the effective mass, E is the energy of the carrier, and $\mathbf{F}(E, E')$ is a function of the energy E before, and after the E' interaction with a phonon, where $E' = E \pm \hbar \omega_0$ for absorption (–) and emission (+), respectively.

The phonon occupation number N_q determines how many phonons occupy that specific mode. This is the quantity of interest for this paper, as it essentially determines the HPB effect. An increase in N_q will alter the emission and absorption rates, bringing them closer together, as the relative factor of $\frac{1}{2} \mp \frac{1}{2}$ becomes less and less dominant for larger values of N_q . If the LO emission and absorption rates come closer together, carriers cannot lose their energy accordingly, hence resulting in longer cooling times. This is essentially how the HPB effect translates a nonequilibrium population of LO-phonons into extended carrier cooling times.

In our previous paper, we defined a perovskite-like system by its effective mass m^* , dielectric constants ϵ_0 and ϵ_∞ , and the typical phonon frequency ω_0 .⁵⁰ Our initial conditions consist of a perovskite-like system in thermal equilibrium at room temperature. Our simulations start with an energy pulse of 0.5 eV to model the photoexcitation by a laser. We track all the particle momenta and positions over time, and find the temperature of the entire system by fitting the kinetic energy distribution to a Maxwell–Boltzmann distribution, defined by a temperature.

We perform simulations up to carrier densities of 10^{19} cm^{-3} . Here, particle statistics are no longer accurately described by the classical Maxwell–Boltzmann regime, as one now enters the quantum mechanical Fermi–Dirac regime.⁶⁶ Our main interest lies in high-energy (high temperature) particle

dynamics. At reasonably high temperatures, there are vastly more energy states than particles. Therefore, the majority of states are empty, and the probability of two particles attempting to occupy the same state is negligible. In this limit, the denominator of the Fermi–Dirac statistics approaches $\exp(-E/k_bT)$, which is recognized as the Maxwell–Boltzmann distribution.⁶⁷ The use of Maxwell–Boltzmann statistics is therefore still appropriate.

For the implementation of the HPB effect, the EMC was extended with the algorithm developed by Lugli et al.⁵¹ For a full description of the algorithm we suggest the original literature.^{51,52,68} We present a summary in the Supporting Information and provide the essential equations below.

The dynamic evolution of the LO phonon population is described by the following difference equation:⁶⁸

$$N_q^{t+\Delta t} = N_q^t + g(q)\Delta t - \frac{\Delta t}{\tau_{LO}}[N_q^t - N_0] \quad (3)$$

where $g(q)$ is given by

$$g(q) = \frac{1}{D_{ph}} \cdot [\Gamma_{em}(q) - \Gamma_{abs}(q)] \quad (4)$$

with $\Gamma_{em}(q)$ the LO phonon emission probability, and $\Gamma_{abs}(q)$ the LO phonon absorption probability, and D_{ph} the phonon density of states.

The phonon density of states is given by

$$D_{ph} = \frac{1}{V_{sim}} \cdot \frac{q^2 \Delta q}{2\pi^2} \quad (5)$$

with V_{sim} the simulation volume, q the phonon wavevector, and Δq the cell size of the q -space histogram. Here, we factor in the simulation volume, and use the general expression for the phonon density of states for a symmetric perfect crystal.⁶⁹ Here, Δq is a free parameter and was taken to be 10^6 cm^{-1} . Choosing Δq is a matter of achieving good statistics.⁷⁰ One should not pick Δq to be too small, as now the perturbation of the phonon population will not properly be captured.

During the entirety of the simulation time, one continuously solves eq 3, and updates the scattering rates via eq 2 accordingly, with updated values for N_q .

We commence with the concentration dependence of the HPB effect in Figure 2, for particle densities between $\rho = 10^{16} \text{ cm}^{-3}$ and $\rho = 10^{19} \text{ cm}^{-3}$. Here, the parameters of the perovskite system were given by $m^* = 0.2$, $\epsilon_0 = 30$, $\epsilon_\infty = 10$, and $\omega_0 = 50 \text{ ps}^{-1}$. This system is comparable with a MAPbI₃ system regarding its effective mass and static dielectric constant ϵ_0 , with ϵ_∞ and ω_0 belonging to a lighter halide system. In these simulations, we kept the lifetime of the phonons constant at $\tau_{LO} = 0.1 \text{ ps}$.

We observe that cooling is impacted at a carrier concentration of 10^{18} cm^{-3} , matching what was reported experimentally for when the HPB would start playing a role in MHP systems.⁴ Going up to higher carrier densities ($\rho = 10^{19} \text{ cm}^{-3}$), we observe a dramatic increase in the cooling time.

In Figure 3 we plot the ratio of the absorption over the emission scattering rate Γ_{abs}/Γ_{em} . The HPB effect will increase the phonon occupation number to values above its equilibrium value, bringing the emission and absorption scattering rates closer together (See eq 2).

At a high particle density ($\rho = 10^{19} \text{ cm}^{-3}$), Γ_{abs}/Γ_{em} is very close to unity, and remains so for the entirety of the simulation time. A significant number of phonons are generated, severely

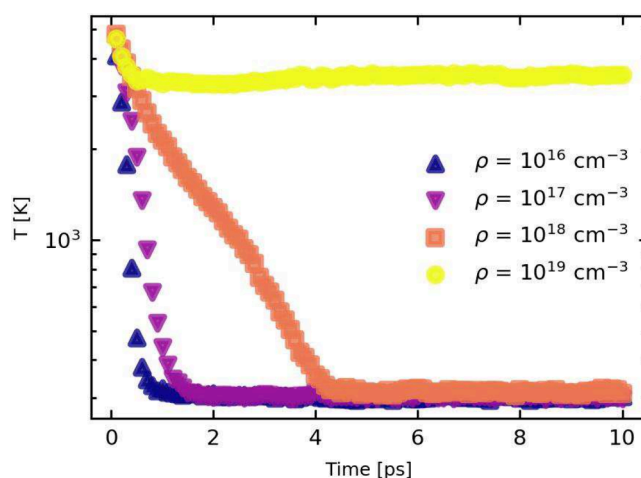


Figure 2. Carrier cooling times for different particle densities ranging from $\rho = 10^{16} \text{ cm}^{-3}$ to $\rho = 10^{19} \text{ cm}^{-3}$. T corresponds the carrier temperature.

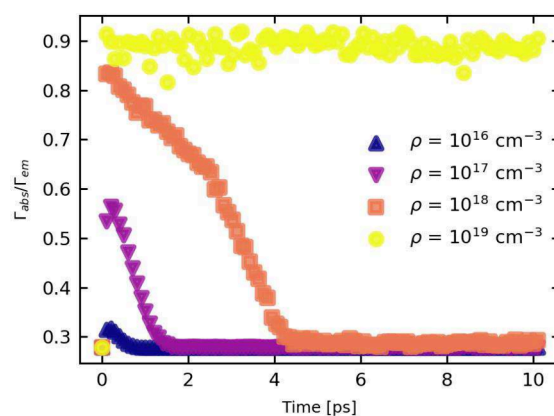


Figure 3. Ratio of the absorption and emission scattering rate for different particle densities ranging from $\rho = 10^{16} \text{ cm}^{-3}$ to $\rho = 10^{19} \text{ cm}^{-3}$.

hindering the system's cooling process. This stretches the cooling time by orders of magnitude, well beyond the LO phonon lifetime τ_{op} . The carrier reabsorption rate is in an absolute sense much larger than the optical phonon decay rate. LO phonons are reabsorbed before they have a chance to decay.

By fitting an exponential to the data of Figure 2, we can obtain a measure for the cooling time for different particle densities, provided in Figure 4. We observe a strong nonlinear increase, illustrating the effect of an increasing reabsorption rate.

What is clear from these results is that a small variation in carrier density will yield significantly different outcomes for the carrier cooling time. In their central study regarding the hot phonon bottleneck in perovskites, Yang et al. show for MAPbI₃, an increase in carrier density from $\rho = 1.5 \times 10^{18} \text{ cm}^{-3}$ to $\rho = 6 \times 10^{18} \text{ cm}^{-3}$, corresponds to more than an order of magnitude increase in the cooling time from around 3 ps to approximately 80 ps.⁶ This corresponds quite well with our findings, and highlights the potential of the HPB effect.

This point is not only an important statement regarding the potential for future HCSC applications, but also of relevance in explaining the variation in experimentally measured cooling

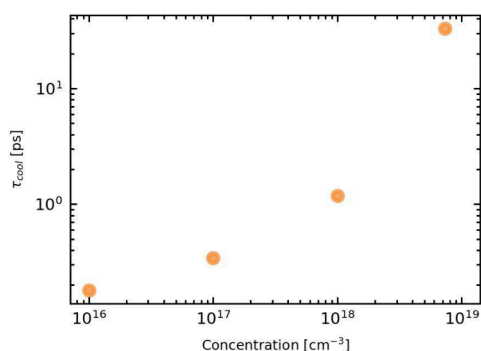


Figure 4. Cooling time vs concentration for $\rho = 10^{16} \text{ cm}^{-3}$ up to $\rho = 10^{19} \text{ cm}^{-3}$ with $\tau_{op} = 0.1 \text{ ps}$. We observe a nonlinear increase in the cooling time with increasing particle density.

times. Only a small uncertainty in the reported pump fluence would result in very different carrier cooling times.

In Figure 5 the dependence of the HPB effect on τ_{LO} is provided. The simulations were performed on a similar

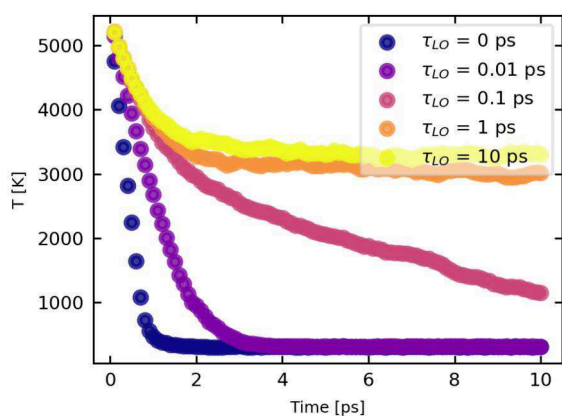


Figure 5. Carrier cooling times for different values of the phonon lifetime τ_{LO} ranging from 0 to 10 ps at a carrier density of $\rho = 10^{18} \text{ cm}^{-3}$.

perovskite-like system ($m^* = 0.15$, $\epsilon_0 = 30$, $\epsilon_\infty = 10$, and $\omega_0 = 31 \text{ ps}^{-1}$), at a particle density of $\rho = 10^{18} \text{ cm}^{-3}$. Cooling times start extending between $\tau_{LO} = 0.1$ and 1 ps, comparable with experimental values found for perovskites.^{7,43} For even longer LO lifetimes τ_{LO} , one can observe that we can elongate the cooling times significantly.

Phonon lifetimes can be impacted by altering the halide composition of the perovskite.⁷¹ However, by comparing three Pb compounds, Leguy et al. show that a change of halide does not so much alter the optical modes, which couple most strongly to the carriers.⁷¹ The authors do point out that increased coupling between the organic and inorganic sublattices leads to a broadening of the Raman peaks.⁷¹ This broadening, characterized by the full-width half-maximum, is inversely proportional to the associated phonon lifetime. Therefore, one could attempt to limit the interaction between the organic and inorganic sublattices. This could be achieved for example by the substitution of an inorganic A-site cation.^{72,73}

Another way to increase the phonon lifetime is by finding a material with a phononic band gap.⁷⁴ Reports have found evidence of a phononic bandgap in lead-based perovskites, suppressing the Klemens decay, as a main decay channel for

LO phonons.^{7,75} A phononic band gap arises from the large difference between the anion and cation masses.^{36,76} This could be further explored by the substitution of a heavier B-site cation,⁷⁷ or lighter halide.⁷⁸ An increase of τ_{LO} to only a few ps, would have very significant effects on the carrier cooling time.

Finally, also up-conversion of other types of phonons back to LO phonons (Reversal of stage 2 in the introduction) must be noted. Up-conversion of acoustic phonons was already mentioned by Yang et al.,³⁶ and more recently by Sekiguchi et al., via excitation of TO phonons.¹⁰ Strong phonon–phonon interactions arise due to a high degree of anharmonicity, originating from the soft Pb–I cage.¹⁰ This results in very short acoustic phonon lifetimes, and therefore a higher probability for up-conversion.^{36,79,80} A further exploration of materials with ultralow thermal conductivity is therefore worthwhile.

Finally, we have investigated the role of the typical phonon frequency ω_0 , shown in Figure 6, for the same perovskite-like system ($m^* = 0.15$, $\epsilon_0 = 30$, $\epsilon_\infty = 10$) at $\rho = 10^{18} \text{ cm}^{-3}$, with $\tau_{LO} = 0.1 \text{ ps}$.

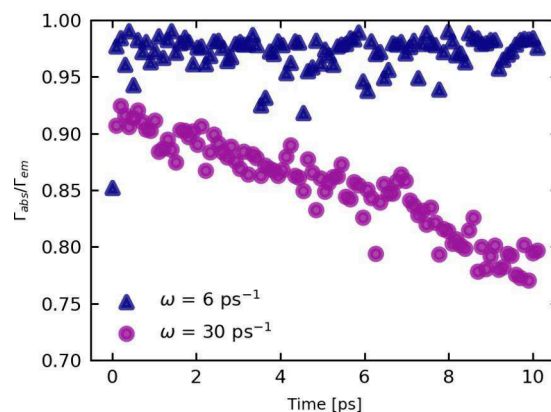


Figure 6. Ratio of the absorption and the emission scattering rate for different typical phonon frequencies $\omega_0 = 6 \text{ ps}^{-1}$ and $\omega_0 = 30 \text{ ps}^{-1}$.

From Figure 6, we observe that for a smaller frequency $\omega_0 = 6 \text{ ps}^{-1}$, the ratio Γ_{abs}/Γ_{em} edges much closer to unity. The HPB effect is shown to be more prominent in lower frequency systems.

The role of the typical phonon frequency ω_0 is not entirely trivial. The quantity returns in the carrier–phonon scattering rate twice. Directly via $\sim \omega_0$ (see eq 2): As the LO phonon energy is smaller, more phonons must be emitted before carriers end up in their respective band edges. However, also in a more subtle, indirect way, via the phonon occupation number N_q . After reaching the peak, the phonon occupation number will relax back to its equilibrium value, which is given by

$$N_0 = \frac{1}{e^{\hbar\omega_0/k_b T_L} - 1} \quad (6)$$

This quantity will be large, for a smaller value of ω_0 , and thus the ratio Γ_{abs}/Γ_{em} will be smaller in equilibrium. Hence, carrier cooling is in general less efficient for systems with smaller values of ω_0 . Additionally, we show here that the HPB effect will be more effective for systems with a smaller typical phonon frequency ω_0 . It is therefore highly fruitful to have a material possessing a small LO-phonon frequency. A possible way to reach smaller LO phonon energies is by switching from a lighter (Cl^-) to a heavier (I^-) halide.^{74,81}

Our study shows how one can significantly extend carrier cooling times by a combined optimization of the carrier concentration, LO phonon lifetime, and LO phonon frequency. Regarding HCSCs care should be taken. On one hand, the need for high carrier concentrations bodes well with the necessity of requiring fast thermalisation to repopulate the extraction levels.⁸² On the other hand, this would raise serious issues with material integrity and device stability.⁷⁸

Finally, at high carrier densities, Auger recombination will also start playing a role.^{7,83} In order to capture the potential of the HPB effect, without experiencing too much interference of Auger recombination, no extreme carrier densities should be used. Our results show that already at densities around $\rho \sim 10^{18}$, a significant boost in cooling time could be obtained by the HPB effect.

We present an investigation of the hot phonon bottleneck (HPB) effect in metal halide perovskites using ensemble Monte Carlo simulations. We have shown, by studying the carrier concentration, LO-phonon lifetime, and LO-phonon frequency, how the HPB effect can extend cooling times by orders of magnitude, far beyond the LO phonon lifetime. Our study connects these findings to concrete chemical compositions for metal halide perovskites, and shows that the HPB effect could play a key role for future HCSC applications.

■ ASSOCIATED CONTENT

Supporting Information

The Supporting Information is available free of charge at <https://pubs.acs.org/doi/10.1021/acs.jpcllett.4c03133>.

Extended overview of EMC and hot phonon bottleneck methodology (PDF)

■ AUTHOR INFORMATION

Corresponding Author

L.J.A. Koster – Zernike Institute for Advanced Materials, University of Groningen, 9747 AG Groningen, The Netherlands; orcid.org/0000-0002-6558-5295; Email: l.j.a.koster@rug.nl

Authors

T. Faber – Zernike Institute for Advanced Materials, University of Groningen, 9747 AG Groningen, The Netherlands; orcid.org/0009-0001-5448-291X

L. Filipovic – CDL for Multi-Scale Process Modeling of Semiconductor Devices and Sensors at the Institute for Microelectronics, TU Wien, 1040 Vienna, Austria; orcid.org/0000-0003-1687-5058

Complete contact information is available at: <https://pubs.acs.org/doi/10.1021/acs.jpcllett.4c03133>

Notes

The authors declare no competing financial interest.

■ ACKNOWLEDGMENTS

The authors would like to thank the Center for Information Technology of the University of Groningen for their support and for providing access to the Peregrine high performance computing cluster, the Zernike Institute for Advanced Materials for funding. The financial support by the Austrian Federal Ministry of Labour and Economy and the National Foundation for Research, Technology and Development and

the Christian Doppler Research Association is gratefully acknowledged.

■ REFERENCES

- (1) Kojima, A.; Teshima, K.; Shirai, Y.; Miyasaka, T. Organometal Halide Perovskites as Visible-Light Sensitizers for Photovoltaic Cells. *J. Am. Chem. Soc.* **2009**, *131*, 6050.
- (2) Lee, M. M.; Teuscher, J.; Miyasaka, T.; Murakami, T. N.; Snaith, H. J. Efficient Hybrid Solar Cells Based on Meso-Superstructured Organometal Halide Perovskites. *Science* **2012**, *338*, 643.
- (3) National Renewable Energy Laboratory. Best Research-Cell Efficiency Chart, 2024. <https://www.nrel.gov/pv/cell-efficiency.html>, Accessed: April 1, 2024.
- (4) Fu, J.; Ramesh, S.; Melvin Lim, J. W.; Sum, T. C. Carriers, Quasiparticles, and Collective Excitations in Halide Perovskites. *Chem. Rev.* **2023**, *123*, 8154.
- (5) Conibeer, G.; Shrestha, S.; Huang, S.; Patterson, R.; Xia, H.; Feng, Y.; Zhang, P.; Gupta, N.; Tayebjee, M.; Smyth, S.; et al. Hot Carrier Solar Cell Absorber Prerequisites and Candidate Material Systems. *Sol. Energy Mater. Sol. Cells* **2015**, *135*, 124.
- (6) Yang, Y.; Ostrowski, D. P.; France, R. M.; Zhu, K.; Van De Lagemaat, J.; Luther, J. M.; Beard, M. C. Observation of a Hot-Phonon Bottleneck in Lead-Iodide Perovskites. *Nat. Photonics* **2016**, *10*, 53.
- (7) Fu, J.; Xu, Q.; Han, G.; Wu, B.; Huan, C. H. A.; Leek, M. L.; Sum, T. C. Hot Carrier Cooling Mechanisms in Halide Perovskites. *Nat. Commun.* **2017**, *8*, 1300.
- (8) Price, M. B.; Butkus, J.; Jellicoe, T. C.; Sadhanala, A.; Briane, A.; Halpert, J. E.; Broch, K.; Hodgkiss, J. M.; Friend, R. H.; Deschler, F. Hot Carrier Cooling and Photoinduced Refractive Index Changes in Organic-Inorganic Lead Halide Perovskites. *pn. Commun.* **2015**, *6*, 8420.
- (9) Monti, M.; Jayawardena, K. I.; Butler-Caddle, E.; Bandara, R. M.; Woolley, J. M.; Staniforth, M.; Silva, S. R. P.; Lloyd-Hughes, J. Hot Carriers in Mixed Pb-Sn Halide Perovskite Semiconductors Cool Slowly While Retaining Their Electrical Mobility. *Phys. Rev. B* **2020**, *102*, 245204.
- (10) Sekiguchi, F.; Hirori, H.; Yumoto, G.; Shimazaki, A.; Nakamura, T.; Wakamiya, A.; Kanemitsu, Y. Enhancing the Hot-Phonon Bottleneck Effect in a Metal Halide Perovskite by Terahertz Phonon Excitation. *Phys. Rev. Lett.* **2021**, *126*, 077401.
- (11) Verkamp, M.; Leveillee, J.; Sharma, A.; Lin, M.-F.; Schleife, A.; Vura-Weis, J. Carrier-Specific Hot Phonon Bottleneck in CH₃NH₃PbI₃ Revealed by Femtosecond XUV Absorption. *J. Am. Chem. Soc.* **2021**, *143*, 20176.
- (12) Nie, Z.; Gao, X.; Ren, Y.; Xia, S.; Wang, Y.; Shi, Y.; Zhao, J.; Wang, Y. Harnessing Hot Phonon Bottleneck in Metal Halide Perovskite Nanocrystals via Interfacial Electron-Phonon Coupling. *Nano Lett.* **2020**, *20*, 4610.
- (13) Hopper, T. R.; Gorodetsky, A.; Frost, J. M.; Müller, C.; Lovrincic, R.; Bakulin, A. A. Ultrafast Intraband Spectroscopy of Hot-Carrier Cooling in Lead-Halide Perovskites. *ACS Energy Letters* **2018**, *3*, 2199.
- (14) Papagiorgis, P.; Protesescu, L.; Kovalenko, M. V.; Othonos, A.; Itskos, G. Long-lived Hot Carriers in Formamidinium Lead Iodide Nanocrystals. *J. Phys. Chem. C* **2017**, *121*, 12434.
- (15) Chen, J.; Messing, M. E.; Zheng, K.; Pullerits, T. Cation-Dependent Hot Carrier Cooling in Halide Perovskite Nanocrystals. *J. Am. Chem. Soc.* **2019**, *141*, 3532.
- (16) Dai, L.; Ye, J.; Greenham, N. C. Thermalization and Relaxation Mediated by Phonon Management in Tin-Lead Perovskites. *Light: Science & Applications* **2023**, *12*, 208.
- (17) Zhu, H.; Miyata, K.; Fu, Y.; Wang, J.; Joshi, P. P.; Niesner, D.; Williams, K. W.; Jin, S.; Zhu, X.-Y. Screening in Crystalline Liquids Protects Energetic Carriers in Hybrid Perovskites. *Science* **2016**, *353*, 1409.
- (18) Niesner, D.; Zhu, H.; Miyata, K.; Joshi, P. P.; Evans, T. J.; Kudisch, B. J.; Trinh, M. T.; Marks, M.; Zhu, X.-Y. Persistent

- Energetic Electrons in Methylammonium Lead Iodide Perovskite Thin Films. *J. Am. Chem. Soc.* **2016**, *138*, 15717.
- (19) Frost, J. M.; Whalley, L. D.; Walsh, A. Slow Cooling of Hot Polarons in Halide Perovskite Solar Cells. *ACS Energy Letters* **2017**, *2*, 2647.
- (20) Evans, T. J. S.; Miyata, K.; Joshi, P. P.; Maeherlein, S.; Liu, F.; Zhu, X.-Y. Competition Between Hot-Electron Cooling and Large Polaron Screening in CsPbBr₃ Perovskite Single Crystals. *J. Phys. Chem. C* **2018**, *122*, 13724.
- (21) Burgos-Caminal, A.; Moreno-Naranjo, J. M.; Willauer, A. R.; Paraecattil, A. A.; Ajarzadeh, A.; Moser, J.-E. Hot Carrier Mobility Dynamics Unravel Competing Subpicosecond Processes in Lead Halide Perovskites. *J. Phys. Chem. C* **2021**, *125*, 98.
- (22) Li, M.; Bhaumik, S.; Goh, T. W.; Kumar, M. S.; Yantara, N.; Grätzel, M.; Mhaisalkar, S.; Mathews, N.; Sum, T. C. Slow Cooling and Highly Efficient Extraction of Hot Carriers in Colloidal Perovskite Nanocrystals. *Nat. Commun.* **2017**, *8*, 14350.
- (23) Shen, J.-X.; Zhang, X.; Das, S.; Kioupakis, E.; Van de Walle, C. G. Unexpectedly Strong Auger Recombination in Halide Perovskites. *Adv. Energy Mater.* **2018**, *8*, 1801027.
- (24) Fang, H.-H.; Adjokatse, S.; Shao, S.; Even, J.; Loi, M. A. Long-Lived Hot-Carrier Light Emission and Large Blue Shift in Formamidinium Tin Triiodide Perovskites. *Nat. Commun.* **2018**, *9*, 243.
- (25) van de Ven, L. J. M.; Tekelenburg, E. K.; Pitaro, M.; Pinna, J.; Loi, M. A. Cation Influence on Hot-Carrier Relaxation in Tin Triiodide Perovskite Thin Films. *ACS Energy Letters* **2024**, *9*, 992.
- (26) Yin, J.; Maity, P.; Naphade, R.; Cheng, B.; He, J.-H.; Bakr, O. M.; Brédas, J.-L.; Mohammed, O. F. Tuning Hot Carrier Cooling Dynamics by Dielectric Confinement in Two-Dimensional Hybrid Perovskite Crystals. *ACS Nano* **2019**, *13*, 12621.
- (27) Li, M.; Begum, R.; Fu, J.; Xu, Q.; Koh, T. M.; Veldhuis, S. A.; Grätzel, M.; Mathews, N.; Mhaisalkar, S.; Sum, T. C. Low Threshold and Efficient Multiple Exciton Generation in Halide Perovskite Nanocrystals. *Nat. Commun.* **2018**, *9*, 4197.
- (28) Dai, L.; Deng, Z.; Auras, F.; Goodwin, H.; Zhang, Z.; Walmsley, J. C.; Bristowe, P. D.; Deschler, F.; Greenham, N. C. Slow Carrier Relaxation in Tin-Based Perovskite Nanocrystals. *Nat. Photonics* **2021**, *15*, 696.
- (29) Pötz, W. Hot-Phonon Effects in Bulk GaAs. *Phys. Rev. B* **1987**, *36*, 5016.
- (30) Prabhu, S. S.; Vengurlekar, A. S. Hot-carrier Energy-Loss Rates in Alloy Semiconductors. *Phys. Rev. B* **1996**, *53*, 7815.
- (31) Prabhu, S.; Vengurlekar, A. Hot-Carrier Energy-Loss Rates in Alloy Semiconductors. *Phys. Rev. B* **1996**, *53*, 7815.
- (32) Prabhu, S.; Vengurlekar, A.; Roy, S.; Shah, J. Nonequilibrium Dynamics of Hot Carriers and Hot Phonons in CdSe and GaAs. *Phys. Rev. B* **1995**, *51*, 14233.
- (33) Choi, C.; Kwon, Y.; Krasinski, J.; Park, G.; Setlur, G.; Song, J.; Chang, Y. Ultrafast Carrier Dynamics in a Highly Excited GaN Epilayer. *Phys. Rev. B* **2001**, *63*, 115315.
- (34) Pugnet, M.; Collet, J.; Cornet, A. Cooling of Hot Electron-Hole Plasmas in the Presence of Screened Electron-Phonon Interactions. *Solid State Commun.* **1981**, *38*, 531.
- (35) Kumekov, S.; Perel, V. Energy Relaxation of the Electron-Phonon System of a Semiconductor under Static and Dynamic Conditions. *Soviet Journal of Experimental and Theoretical Physics* **1988**, *67*, 193.
- (36) Yang, J.; Wen, X.; Xia, H.; Sheng, R.; Ma, Q.; Kim, J.; Tapping, P.; Harada, T.; Kee, T. W.; Huang, F.; et al. Acoustic-Optical Phonon Up-Conversion and Hot-Phonon Bottleneck in Lead-Halide Perovskites. *Nat. Commun.* **2017**, *8*, 14120.
- (37) Fröhlich, H.; Mott, N. F. Theory of Electrical Breakdown in Ionic Crystals. II. *Proceedings of the Royal Society of London. Series A. Mathematical and Physical Sciences* **1939**, *172*, 94.
- (38) Wright, A. D.; Verdi, C.; Milot, R. L.; Eperon, G. E.; Pérez-Osorio, M. A.; Snaith, H. J.; Giustino, F.; Johnston, M. B.; Herz, L. M. Electron-Phonon Coupling in Hybrid Lead Halide Perovskites. *Nat. Commun.* **2016**, *7*, 11755.
- (39) Klemens, P. G. Anharmonic Decay of Optical Phonons. *Phys. Rev.* **1966**, *148*, 845.
- (40) Ridley, B. K. Electron Scattering by Confined LO Polar Phonons in a Quantum Well. *Phys. Rev. B* **1989**, *39*, 5282.
- (41) König, D.; Casalenuovo, K.; Takeda, Y.; Conibeer, G.; Guillemoles, J.-F.; Patterson, R.; Huang, L.; Green, M. Hot Carrier Solar Cells: Principles, Materials and Design. *Physica E: Low-dimensional Systems and Nanostructures* **2010**, *42*, 2862.
- (42) Shah, J. *Ultrafast Spectroscopy of Semiconductors and Semiconductor Nanostructures*; Springer Science & Business Media, 1996; vol. 115.
- (43) Jung, Y.; Lee, W.; Han, S.; Kim, B.-S.; Yoo, S.-J.; Jang, H. Thermal Transport Properties of Phonons in Halide Perovskites. *Adv. Mater.* **2023**, *35*, 2204872.
- (44) Jacoboni, C.; Lugli, P. *The Monte Carlo Method for Semiconductor Device Simulation, Computational Microelectronics*. Springer, 2011.
- (45) Jacoboni, C.; Reggiani, L. The Monte Carlo method for the Solution of Charge Transport in Semiconductors with Applications to Covalent Materials. *Rev. Mod. Phys.* **1983**, *55*, 645.
- (46) Ferry, D. K. The ensemble Monte Carlo method. *Hot Carriers in Semiconductors* **2021**, 7-1-7-49.
- (47) Tomizawa, K. *Numerical Simulation of Submicron Semiconductor Devices*; Artech House Publishers, 1993.
- (48) Hockney, R.; Eastwood, J. *Computer Simulation Using Particles*; CRC Press, 1988.
- (49) Kosina, H.; Nedjalkov, M.; Selberherr, S. Theory of the Monte Carlo Method for Semiconductor Device Simulation. *IEEE Trans. Electron Devices* **2000**, *47*, 1898.
- (50) Faber, T.; Filipovic, L.; Koster, L. J. A. The Role of Thermalization in the Cooling Dynamics of Hot Carrier Solar Cells. *Solar RRL* **2023**, *7*, 2300140.
- (51) Lugli, P.; Jacoboni, C.; Reggiani, L.; Kocevar, P. Monte Carlo Algorithm for Hot Phonons in Polar Semiconductors. *Appl. Phys. Lett.* **1987**, *50*, 1251.
- (52) Lugli, P.; Bordone, P.; Reggiani, L.; Rieger, M.; Kocevar, P.; Goodnick, S. M. Monte Carlo Studies of Nonequilibrium Phonon Effects in Polar Semiconductors and Quantum Wells. I. Laser Photoexcitation. *Phys. Rev. B* **1989**, *39*, 7852.
- (53) Joshi, R. P.; Grondin, R. O.; Ferry, D. K. Monte Carlo Simulation of Electron-Hole Thermalization in Photoexcited Bulk Semiconductors. *Phys. Rev. B* **1990**, *42*, 5685.
- (54) Dür, M.; Goodnick, S. M.; Lugli, P. Monte Carlo Simulation of Intersubband Relaxation in Wide, Uniformly Doped GaAs/Al_xGa_{1-x}As Quantum Wells. *Phys. Rev. B* **1996**, *54*, 17794.
- (55) Zou, Y.; Esmailpour, H.; Suchet, D.; Guillemoles, J.-F.; Goodnick, S. M. The Role of Nonequilibrium LO phonons, Pauli exclusion, and Intervalley Pathways on the Relaxation of Hot Carriers in InGaAs/InGaAsP Multi-Quantum-Wells. *Sci. Rep.* **2023**, *13*, 5601.
- (56) Iaru, C. M.; Brodu, A.; van Hoof, N. J.; Ter Huurne, S. E.; Buhut, J.; Montanarella, F.; Buhut, S.; Christianen, P. C.; Vanmaekelbergh, D.; de Mello Donega, C.; et al. Fröhlich Interaction Dominated by a Single Phonon Mode in CsPbBr₃. *Nat. Commun.* **2021**, *12*, 5844.
- (57) Poncé, S.; Schlipf, M.; Giustino, F. Origin of Low Carrier Mobilities in Halide Perovskites. *ACS Energy Letters* **2019**, *4*, 456.
- (58) Schlipf, M.; Poncé, S.; Giustino, F. Carrier Lifetimes and Polaronic Mass Enhancement in the Hybrid Halide Perovskite CH₃NH₃PbI₃ from Multiphonon Fröhlich Coupling. *Phys. Rev. Lett.* **2018**, *121*, 086402.
- (59) Hellwarth, R. W.; Biaggio, I. Mobility of an Electron in a Multimode Polar Lattice. *Phys. Rev. B* **1999**, *60*, 299.
- (60) Lan, Y.; Dringoli, B. J.; Valverde-Chávez, D. A.; Ponseca, C. S.; Sutton, M.; He, Y.; Kanatzidis, M. G.; Cooke, D. G. Ultrafast Correlated Charge and Lattice Motion in a Hybrid Metal Halide Perovskite. *Science Advances* **2019**, *5*, No. eaaw5558.
- (61) Frost, J. M. Calculating Polaron Mobility in Halide Perovskites. *Phys. Rev. B* **2017**, *96*, 195202.

- (62) Irvine, L. A.; Walker, A. B.; Wolf, M. J. Quantifying Polaronic Effects on the Scattering and Mobility of Charge Carriers in Lead Halide Perovskites. *Phys. Rev. B* **2021**, *103*, L220305.
- (63) Ferreira, A.; Paofai, S.; Létoublon, A.; Ollivier, J.; Raymond, S.; Hehlen, B.; Rufflé, B.; Cordier, S.; Katan, C.; Even, J.; et al. Direct Evidence of Weakly Dispersed and Strongly Anharmonic Optical Phonons in Hybrid Perovskites. *Communications Physics* **2020**, *3*, 48.
- (64) Gollner, L.; Steiner, R.; Filipovic, L. Vienna-EMC. <https://github.com/ViennaTools/ViennaEMC>, 2023, Accessed: April 1, 2024.
- (65) Blanchard, P.; Bramas, B.; Coulaud, O.; Darve, E. F.; Dupuy, L.; Etcheverry, A.; Sylvand, G. ScalFMM: A Generic Parallel Fast Multipole Library. <https://gitlab.inria.fr/solverstack/ScalFMM>, 2017, Accessed: April 1, 2024.
- (66) Zebarjadi, M.; Bulutay, C.; Esfarjani, K.; Shakouri, A. Monte Carlo Simulation of Degenerate Semiconductors. *Appl. Phys. Lett.* **2007**, *90*, 092111.
- (67) Vincenti, W.; Kruger, C. *Introduction to Physical Gas Dynamics*; Wiley, 1965.
- (68) Lugli, P. Hot Phonon Dynamics. *Solid-State Electron.* **1988**, *31*, 667.
- (69) Kittel, C.; McEuen, P. *Introduction to Solid State Physics*; Wiley, 2018.
- (70) Ferry, D. *Semiconductor Transport*; CRC Press, 2016.
- (71) Leguy, A. M. A.; Goñi, A. R.; Frost, J. M.; Skelton, J.; Brivio, F.; Rodríguez-Martínez, X.; Weber, O. J.; Pallipurath, A.; Alonso, M. L.; Campoy-Quiles, M.; Weller, M. T.; Nelson, J.; Walsh, A.; Barnes, P. R. F. Dynamic Disorder, Phonon Lifetimes, and the Assignment of Modes to the Vibrational Spectra of Methylammonium Lead Halide Perovskites. *Phys. Chem. Chem. Phys.* **2016**, *18*, 27051.
- (72) Ghosh, D.; Welch, E.; Neukirch, A. J.; Zakhidov, A.; Tretiak, S. Polarons in Halide Perovskites: a Perspective. *J. Phys. Chem. Lett.* **2020**, *11*, 3271.
- (73) Gallop, N. P.; Selig, O.; Giubertoni, G.; Bakker, H. J.; Rezus, Y. L. A.; Frost, J. M.; Jansen, T. L. C.; Lovrincic, R.; Bakulin, A. A. Rotational Cation Dynamics in Metal Halide Perovskites: Effect on Phonons and Material Properties. *J. Phys. Chem. Lett.* **2018**, *9*, 5987.
- (74) Kahmann, S.; Loi, M. Hot Carrier Solar Cells and the Potential of Perovskites for Breaking the Shockley-Queisser limit. *Journal of Materials Chemistry C* **2019**, *7*, 2471.
- (75) Kim, H.; Hunger, J.; Cánovas, E.; Karakus, M.; Mics, Z.; Grechko, M.; Turchinovich, D.; Parekh, S. H.; Bonn, M. Direct Observation of Mode-Specific Phonon-Band Gap Coupling in Methylammonium Lead Halide Perovskites. *Nat. Commun.* **2017**, *8*, 687.
- (76) Conibeer, G.; Ekins-Daukes, N.; Guillemoles, J.-F.; König, D.; Cho, E.-C.; Jiang, C.-W.; Shrestha, S.; Green, M. Progress on Hot Carrier Cells. *Solar Energy Materials and Solar Cells* **2009**, *93*, 713.
- (77) Chatterjee, S.; Pal, A. J. Influence of Metal Substitution on Hybrid Halide Perovskites: Towards Lead-Free Perovskite Solar Cells. *Journal of Materials Chemistry A* **2018**, *6*, 3793.
- (78) Li, M.; Fu, J.; Xu, Q.; Sum, T. C. Slow Hot-Carrier Cooling in Halide Perovskites: Prospects for Hot-Carrier Solar Cells. *Adv. Mater.* **2019**, *31*, 1802486.
- (79) Gold-Parker, A.; Gehring, P. M.; Skelton, J. M.; Smith, I. C.; Parshall, D.; Frost, J. M.; Karunadasa, H. I.; Walsh, A.; Toney, M. F. Acoustic Phonon Lifetimes Limit Thermal Transport in Methylammonium Lead Iodide. *Proc. Natl. Acad. Sci. U. S. A.* **2018**, *115*, 11905.
- (80) Katan, C.; Mohite, A. D.; Even, J. Entropy in Halide Perovskites. *Nat. Mater.* **2018**, *17*, 377.
- (81) Savill, K. J.; Ulatowski, A. M.; Herz, L. M. Optoelectronic Properties of Tin–Lead Halide Perovskites. *ACS Energy Letters* **2021**, *6*, 2413.
- (82) Takeda, Y.; Motohiro, T.; König, D.; Aliberti, P.; Feng, Y.; Shrestha, S.; Conibeer, G. Practical Factors Lowering Conversion Efficiency of Hot Carrier Solar Cells. *Applied Physics Express* **2010**, *3*, 104301.
- (83) Shen, J.-X.; Zhang, X.; Das, S.; Kioupakis, E.; Van de Walle, C. G. Unexpectedly Strong Auger Recombination in Halide Perovskites. *Adv. Energy Mater.* **2018**, *8*, 1801027.